ESS 5203: Notes 5: Marine Boundary Layers

An old good text: Owen M. Phillips, The Dynamics of the Upper Ocean, CUP, 1966, 1977 (Scott Library)

On-Line availability through library,

BOOK

Air-sea interaction : laws and mechanisms

Csanady, G. T.

2001

Available at Steacie Science & Engineering Library Steacie Stacks (GC 190.2 C73 2001)

Available Online

The near-surface layer of the ocean : structure, dynamics and applications

Soloviev, Alexander, author.; Lukas, Roger, author.

2014

Available Online

Lots of Canadian involvement in Air Sea Interaction, at BIO (Fred Dobson, Stuart Smith), UBC (Paul LeBlond, Robert Stewart) , CCIW (Mark Donelan – then moved to Miami). Also Southampton University, UK, (Henry Charnock, Tom Ellison, John Woods and Jim Salmon, Peter Gent and myself).

Notes from Soloviev, Chapters 1,2

The top 2-3 m of the ocean has the same heat capacity as the entire atmosphere above. Of the penetrating solar radiation, 50% is absorbed within the first 0.5 m of the ocean. Of the breaking surface wave kinetic energy, 50% dissipates within 20% of the significant wave height from the surface. These facts highlight the special role of the near-surface layer of the ocean in the ocean-atmosphere system.

The variety of forcing factors, in combination with nonlinear feedbacks, result in different near-surface regimes. Fedorov and Ginzburg (1988) consider five regimes in the near-surface layer of the ocean:

1) Intensive wind-wave mixing (wind speed at 10 m height above the ocean surface $U_{10} > 8\text{-}10$ m s^{-1});
2) Intensive convection (nighttime, winter, or atmospheric cold fronts);
3) Langmuir circulations (U_{10} from 3 to 10 m s^{-1});
4) Intensive solar heating under low wind and calm weather conditions (U_{10} from 0 to 3-5 m s^{-1});
5) Near-surface freshening due to rain.

Above the water: Drag coefficients $u^{*2} = C_D U_{10}^2$ – the Charnock-Ellison formula ($z_0 = 0.011u^{*2}/g$):

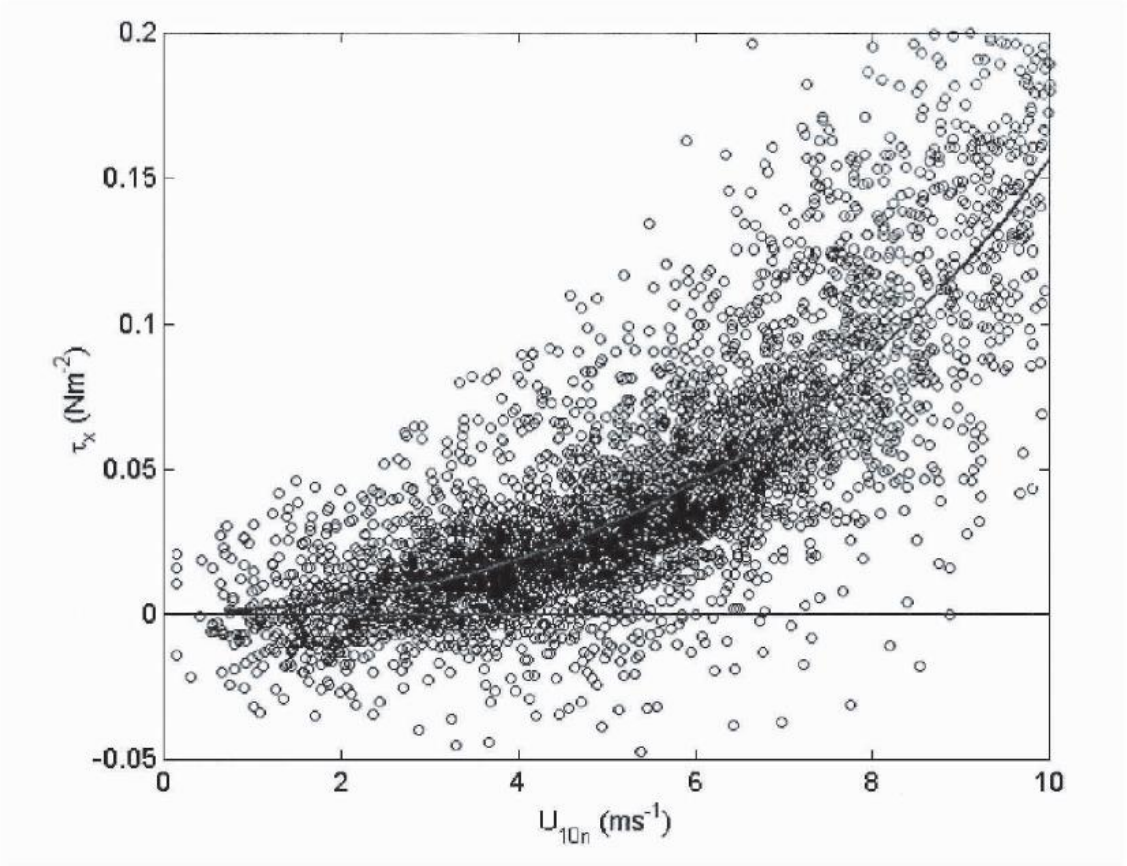

Figure 1-3. Covariance measurements of the streamwise momentum flux (τ_x) as a function of 10 m neutral wind speed. The individual points are nominal 1-hour averages. The solid curve is the COARE 3.0 bulk flux algorithm. Reproduced from Fairall et al. (2003) by permission of American Meteorological Society.

Sea state? Takes time to develop, is there an equilibrium "Fully aroused sea"? And time to decay, sea and swell.

Wave generation by wind. Miles and Phillips mechanisms. Gent and Taylor model.
Grimshaw, 2018

Various mechanisms have been proposed to describe the generation of waves by wind. But despite decades of theoretical research, observations and more recently, detailed numerical simulations, the nature of these mechanisms and their practical applicability remains controversial, see the recent assessments by [12], [16] and [14], and the comprehensive reviews by [1] and [7].

numerical model of the air flow above water waves

P. R. Gent [a1] and P. A. Taylor [a1]

- DOI: https://doi.org/10.1017/S0022112076001158

Published online by Cambridge University Press: 11 April 2006

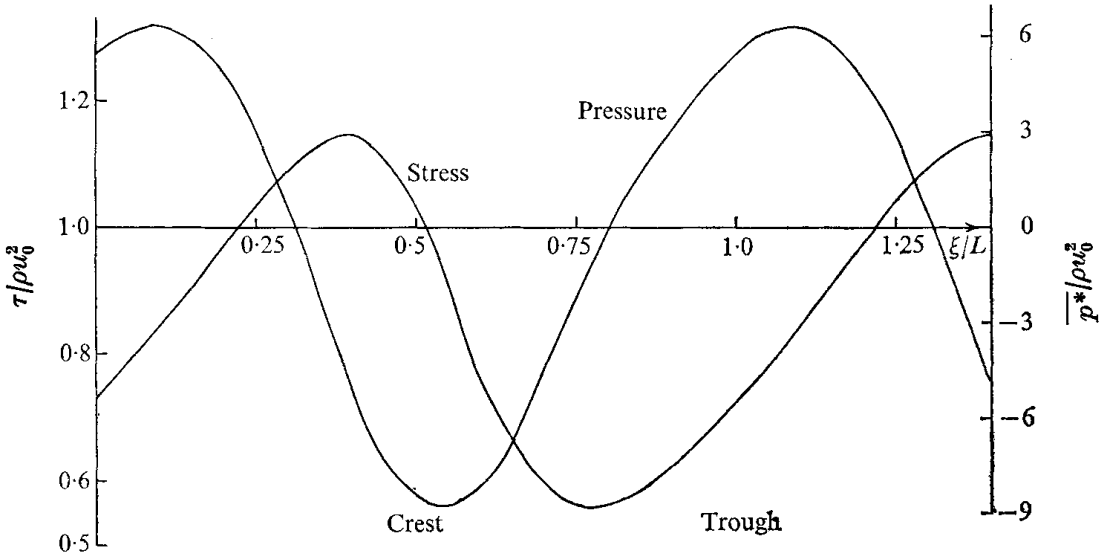

FIGURE 1. Surface pressure and shear stress. $R = 8$, $c = 8u_0$, $ak = 0{\cdot}157$, constant z_0.

Pressure minimum forward of the crest, maximum forward of the trough. So wind can produce a drag on the waves, and transfer momentum and energy. Effects of adding roughness variation.

Gong et al findings on flow over wavy surfaces, Turbulent boundary-layer flow over fixed aerodynamically rough two-dimensional sinusoidal waves

W. Gong, Peter A. Taylor, Andreas Dörnbrack : Published online by Cambridge University Press: 26 April 2006, pp. 1-37, Print publication: 10 April 1996

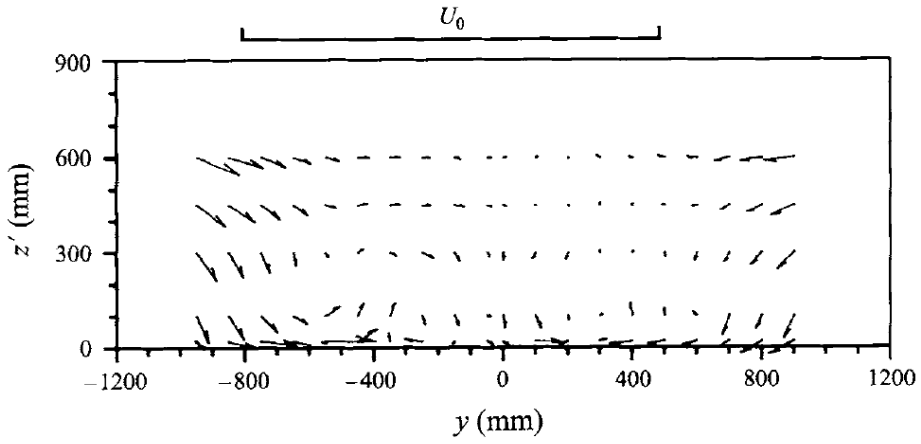

FIGURE 11. Vector plot of secondary flow (V, W) over the 12th crest (relatively smooth-surface case). Horizontal scale above the figure represents U_0 (approximately 10 m s^{-1}).

Maybe this organized flow can add to momentum transfer – an idea still floating around.

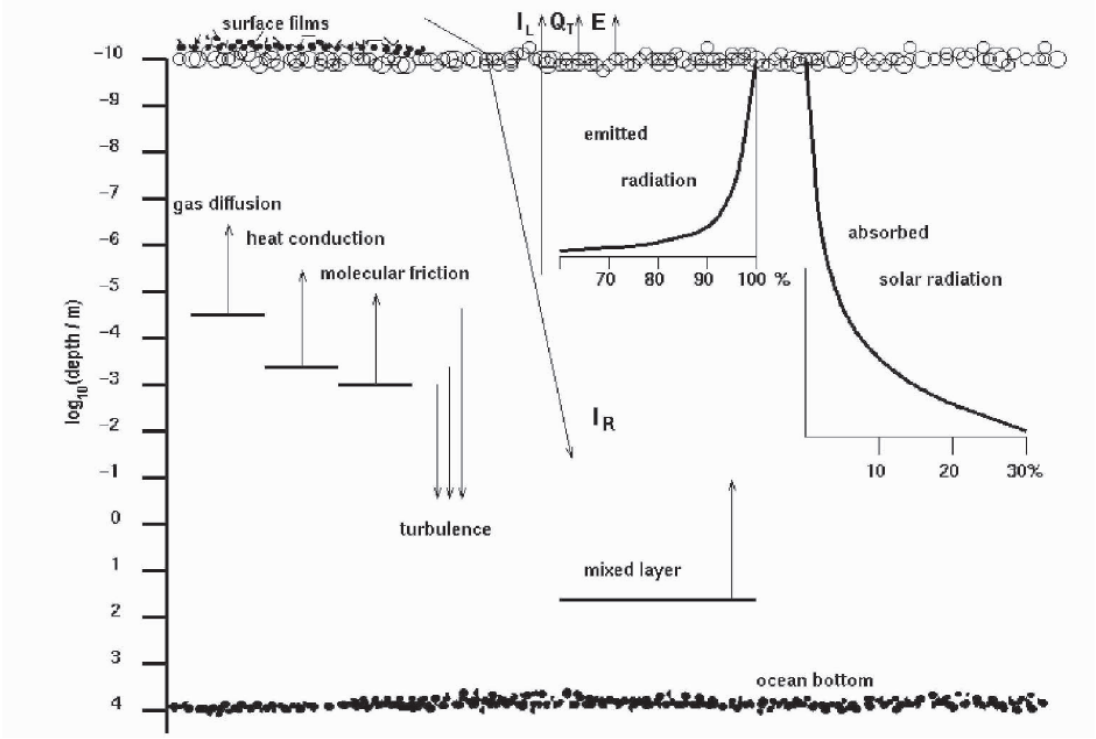

Figure 2-1. Schematic representation of the vertical structure of physical processes related to the sea surface microlayer (Courtesy of Peter Schlüssel, private communication).

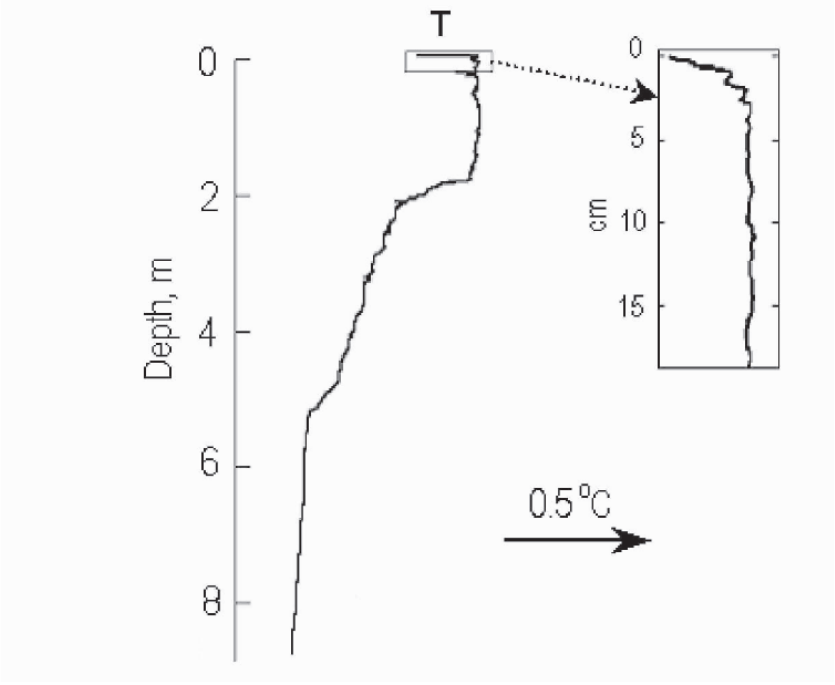

Figure 2-3. An "instantaneous" vertical profile of temperature in the upper ocean taken under low wind speed conditions. (After Soloviev, 1992.)

A sea surface microlayer – molecular diffusion, cool skins, diurnal thermoclines, solar radiation penetration. Surface renewal events.

The renewal concept follows from the idea of intermittent transport of properties across molecular sublayers. Kim et al. (1971) found that the turbulent momentum transport and production in a wall layer take place intermittently in time and space through small-scale bursting motions.

The renewal model developed by Liu and Businger (1975) capitalized on the Kim et al. (1971) result and considered intermittent transport of properties across molecular sublayers. Liu and Businger (1975) developed a method for calculation of average temperature profiles in molecular sublayers by assuming that the sublayers undergo cyclic growth and subsequent destruction. Kudryavtsev and Soloviev (1985) parameterized the transition from free to forced convection in the cool skin using the surface Richardson number Rf_0 as the determining parameter. Soloviev and Schlüssel (1994) incorporated a Keulegan number (Ke) dependence for high wind speed conditions and developed a coupled parameterization for the temperature difference across the cool skin of the ocean and the air-sea gas transfer velocity.

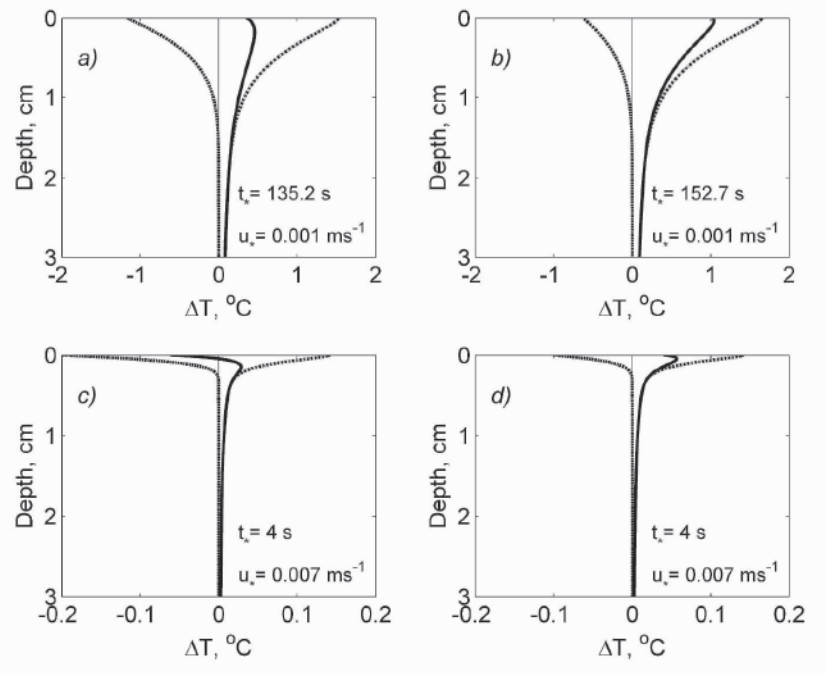

Figure 2-15. Instantaneous vertical temperature profiles in the upper 3 cm of the ocean at the end of the time period between renewal events. The contribution of the solar heating (dash-dotted), surface cooling (dashed), and the combined effect (contiguous) are calculated from a renewal model for (a, c) $Q_0 = 140$ W m^{-2}, $Q_E = 70$ W m^{-2} and (b, d) $Q_0 = 70$ W m^{-2}, $Q_E = 35$ W m^{-2}. The top row (a, b) corresponds to free and the bottom row (c, d) to forced convection regimes. Solar irradiance just below the sea surface $I_{R0} = 1000$ W m^{-2}, water temperature $T_0 = 29$°C, and salinity $S_0 = 36$ psu are the same in all cases. Note the different temperature scale between the top and bottom pairs of diagrams.

A simpler model, from COHERENS,

Afsharian, S., & Taylor, P. A. (2019). On the potential impact of Lake Erie wind farms on water temperatures and mixed-layer depths: Some preliminary 1-D modeling using COHERENS. Journal of Geophysical Research: Oceans, 124, 1736–1749. https://doi.org/10.1029/2018JC014577

Appendix A: COHERENS Details

Tides are not important in Lake Erie and can be neglected. The basic 1-D time-dependent equations in the absence of advection and tide are then given by

$$\frac{\partial u}{\partial t} - fv = \partial\left(\nu_T \frac{\partial u}{\partial z}\right)/\partial z \tag{A1}$$

$$\frac{\partial v}{\partial t} + fu = \partial\left(\nu_T \frac{\partial v}{\partial z}\right)/\partial z \tag{A2}$$

$$\frac{\partial T}{\partial t} = \frac{1}{\rho_0 c_p}\frac{\partial I}{\partial z} + \frac{\partial}{\partial z}\left(\lambda_T \frac{\partial T}{\partial z}\right) \tag{A3}$$

The boundary conditions are

$$\rho_0 \nu_T \left(\frac{\partial u}{\partial z}, \frac{\partial v}{\partial z}\right) = (\tau_{s1}, \tau_{s2}) \tag{A4}$$

$$\rho_0 c_p \lambda_T \left(\frac{\partial T}{\partial z}\right) = -Q_{\text{nsol}} \tag{A5}$$

at the surface, where τ is the surface stress imposed by the wind and Q_{nsol} is the nonsolar heat flux at the surface. The (upward directed) nonsolar heat flux has three components, for example,

$$Q_{\text{nsol}} = Q_{\text{la}} + Q_{\text{se}} + Q_{\text{lw}} \tag{A6}$$

where Q_{la} is the latent heat flux released by evaporation, Q_{se} is the sensible heat flux due to the turbulent transport of temperature across the air/sea interface, and Q_{lw} is the net long-wave radiation (upward directed) at the sea surface. Upwelling long-wave radiation depends on water surface temperature while downwelling is based on the air temperature, cloud cover, and humidity (Gill, 1982). Also, at the bottom

$$\rho_0 \nu_T \left(\frac{\partial u}{\partial z}, \frac{\partial v}{\partial z}\right) = \rho_0 C_{db} \sqrt{u_b^2 + v_b^2}\,(u_b, v_b) \tag{A7}$$

$$\rho_0 c_p \lambda_T \left(\frac{\partial T}{\partial z}\right) = 0 \tag{A8}$$

The solar irradiance in the temperature equation is a significant input and is absorbed within a column using $\lambda_1^{-1} = 10.0$ m and $\lambda_2^{-1} = 0.067$ m which are inverse optical attenuation depths for absorption of long-wave and short-wave solar radiation components, respectively. The infrared fraction of irradiance absorbed at the lake surface is 0.54 (Paulson & Simpson, 1977).

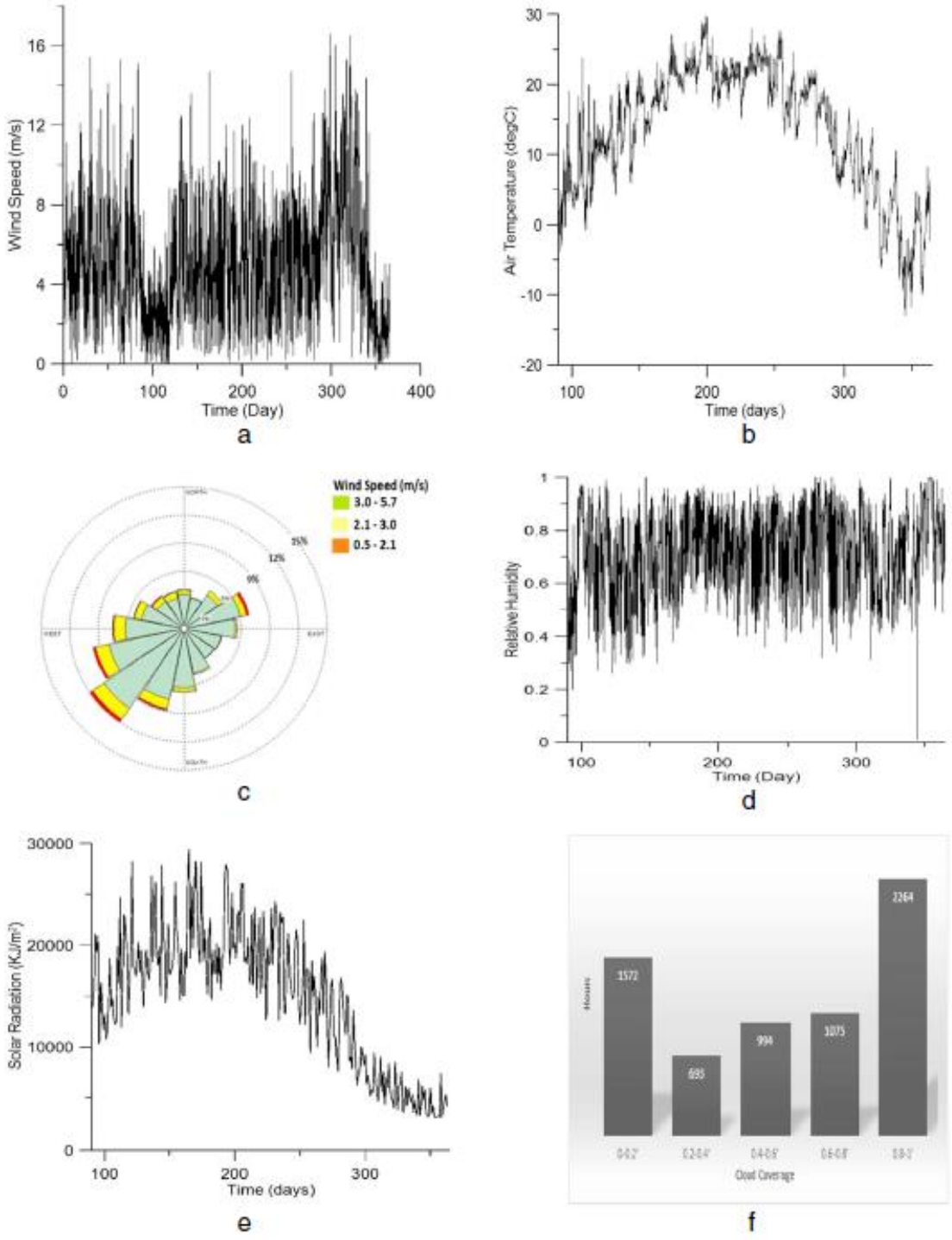

Figure 2. Meteorological data used as input from day of the year 2013, DOY 90–365. (a) Hourly wind speed at 4 m, (b) hourly air temperature at 4 m, (c) hourly wind direction at 4 m, (d) hourly relative humidity, (e) daily-averaged incoming solar radiation, and (f) hourly cloud coverage. Data are from NOAA stations 45005 located at 41°67′N and 82°39′ S and HHLO1 located at 41°40′N, 82°54′W and from Windsor A Ontario station at 42°16′N and 82°57′W.

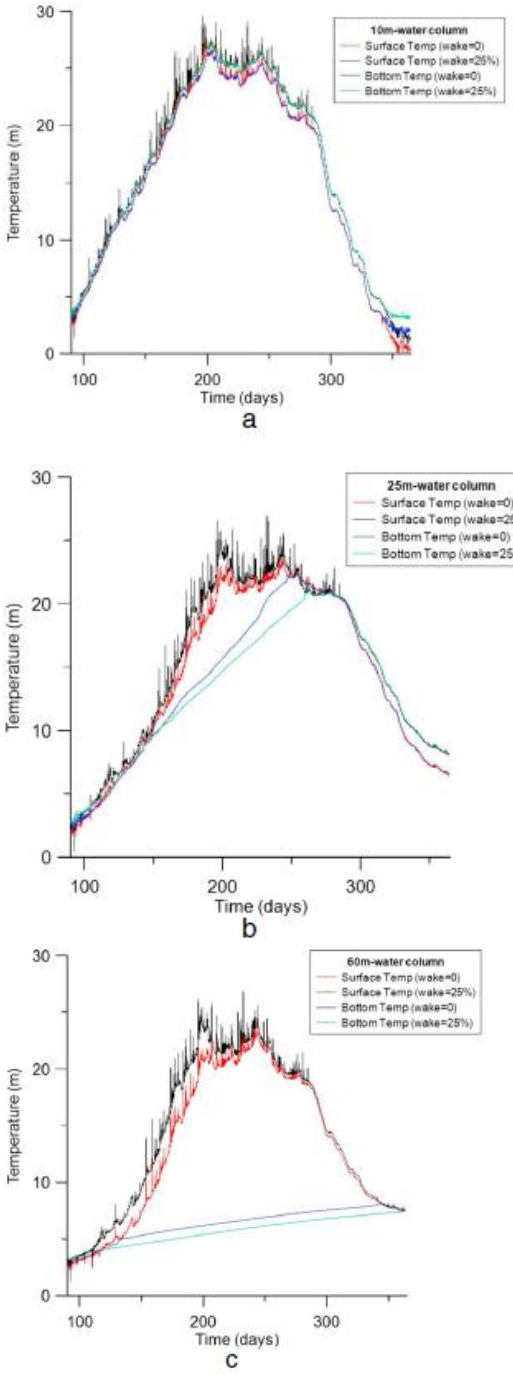

Figure 3. Surface and near-bottom temperatures throughout the 2013 open water season. The 1-D model results for water depths of 10, 25, and 60 m, with measured meteorological input and with a 25% wake reduction in wind speed.

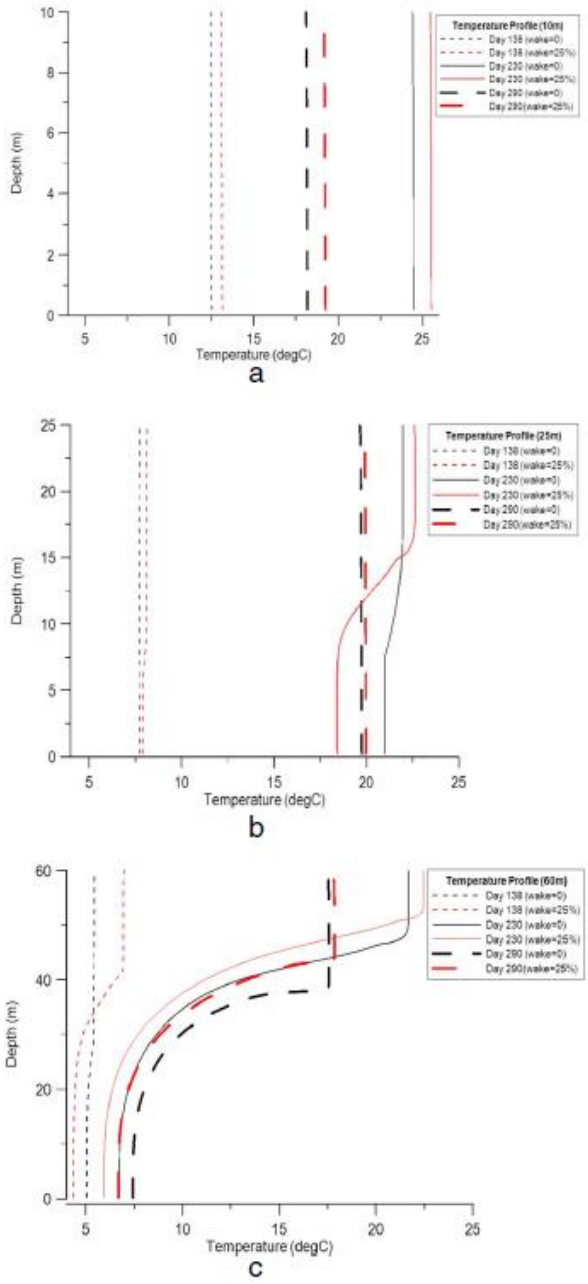

Figure 4. Sample temperature profiles at noon on DOY 138, 230, and 290, for water depth of 10, 25, and 60 m, with and without wake effect wind speed reductions.

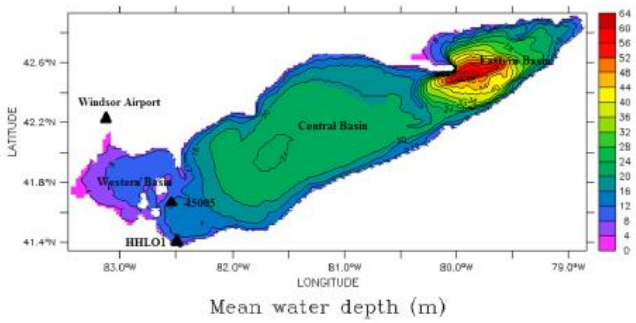

Salinity effects ; evaporation releases salt, increases density. Rain reduces salinity. River outflow situations.
Sediments, sand. Modifies density, affects stratification, a modification of MOST.
From Taylor and Dyer 1977, The Sea. $X = \ln(C/C_0)$.. Modified MOST …

This will integrate to give equilibrium profiles defined by

$$X = -B\zeta - \ln\left[1 + \frac{AB}{(1-B)}(e^{(1-B)\zeta} - 1)\right] \tag{15}$$

The corresponding velocity profiles take the similar form

$$U = \frac{u_*}{\kappa}\left[\zeta + \frac{1}{B}\ln\left\{1 + \frac{AB}{(1-B)}(e^{(1-B)\zeta} - 1)\right\}\right] \tag{16}$$

and are essentially mirror images of the X profiles.

The results given here for velocity and sediment concentration profiles have been previously presented by Barenblatt (1953, 1955) (see Monin and Yaglom, 1971, p. 416 for a brief summary) using Kolmogorov's ideas for closure of the turbulent energy equation. This work seems to have passed unnoticed in the recent Western literature on the subject.

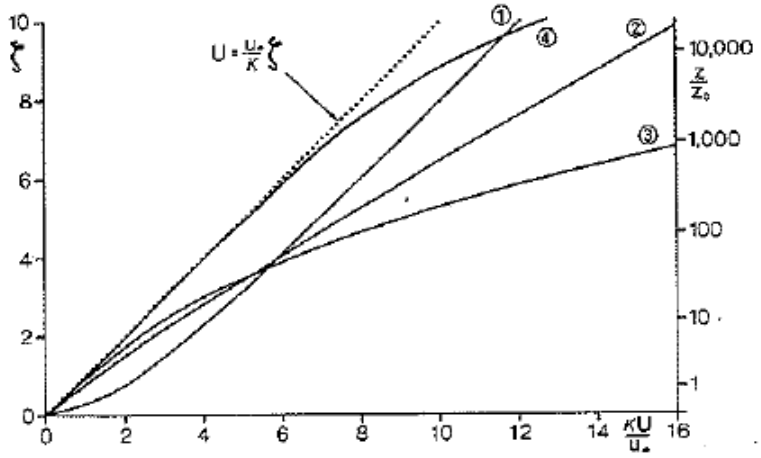

Case 2: $B = 0.56$, $A = 0.32$

These values arise if we set $u_* = 10$ cm/sec, corresponding to a quite strong current, and keep all other parameters as in Case 1. In this case the sediment concentration still falls off quite rapidly away from the bed but as a result of the increasing effectiveness of stratification as we move away from the bed the velocity profile is modified for all z. In particular, for large ζ we have, provided $B < 1$,

$$U \simeq \frac{u_*}{B\kappa}\left[\zeta + \ln\frac{AB}{1-B}\right] \tag{17}$$

Case 1: $B = 1.4$, $A = 5.0$

These values, for moderate flow above quite coarse sandy gravel, are attained if we set $u_* = 4$ cm/sec, $w_s = 2.24$ cm/sec (particle diameter $\simeq 0.02$ cm), $z_0 = 1.0$ cm, and $\gamma C_0 = 0.07$. In this case, with $B > 1$, the sediment concentration falls off rapidly with z and the influence on the velocity profile is confined to the lower layers. At higher elevations the velocity profile retains the same slope as in the sediment free situation.